Prev. Nutr. Food Sci. 2024;29(3):365-375
https://doi.org/10.3746/pnf.2024.29.3.365
ISSN 2287-8602

Effect of the Autoclaving-Cooling Cycle on the Chemical, Morphological, Color, and Pasting Properties of Foxtail Millet Starch

Fitri Electrika Dewi Surawan[1,2], Eni Harmayani[1], Nurliyani[3], and Djagal Wiseso Marseno[1]

[1]Department of Food and Agricultural Product Technology, Faculty of Agricultural Technology and [3]Department of Animal Product Technology, Faculty of Animal Science, Universitas Gadjah Mada, Yogyakarta 55281, Indonesia
[2]Department of Agricultural Technology, Faculty of Agriculture, University of Bengkulu, Bengkulu 38122, Indonesia

ABSTRACT: This study investigated the effect of the autoclaving-cooling (AC) cycle and the starch-to-water ratio on the chemical, morphological, color, and pasting properties of foxtail millet starch to improve its utilization in the food industry. Starch suspensions were prepared using different starch-to-water ratios (i.e., 1:1 and 1:4), with one to three AC cycles for each ratio. Subsequently, the chemical, morphological, color, and pasting properties of native and autoclaved-cooled foxtail millet starch (ACFS) were determined. The results showed that ACFS had higher overall resistant starch (RS) content than native starch. AC treatment reduced the lightness and whiteness index, gelatinization time, and pasting temperature while increasing particle sizes with irregular shapes and surfaces. Starch treated with distilled water at a 1:1 ratio with two AC cycles (1:1-2C) exhibited the highest amylose, starch, and RS contents with stable pasting properties compared with that in other AC treatments. Pasting stability was indicated by the low breakdown viscosity and high trough and final viscosity. The findings suggest that ACFS treated with 1:1-2C could be a stabilizer and functional food.

Keywords: autoclaving-cooling, morphological properties, pasting properties, resistant starch, setaria plant

INTRODUCTION

Foxtail millet (*Setaria italica* (L.) P. Beauv.) is a cereal with favorable properties. Because of its short plant height, quick growing time, and salt and drought tolerance, foxtail millet is valuable in semiarid tropical regions (Doust et al., 2009). Foxtail millet is mostly grown in Indonesia, particularly in the provinces of Bengkulu, South Sumatra, West Java, Papua, East Nusa Tenggara, and West Sulawesi (Miswarti et al., 2014; Ramlah et al., 2020).

Many studies have determined the nutritional composition of foxtail millet (Bhat et al., 2018; Doddamani and Yenagi, 2018) and its potential applications in various food processing technologies. For example, foxtail millet seeds have been used in studies on popping technology (Mishra et al., 2014), bread making (Ballolli et al., 2014), and cereal bar processing (Babu and Mohan, 2023). Furthermore, studies on the isolation methods and characterization of foxtail millet starch (Surawan et al., 2021), its functional properties (Bangoura et al., 2012), and its properties after annealing and ultrasonic modification (Babu et al., 2019) have been reported. However, few studies have characterized foxtail millet starch and investigated the effects of other physical modifications, especially autoclaving-cooling (AC) methods.

Compared with other methods, physical starch modification is preferred because of its convenience, cost-effectiveness, and safety as it does not produce chemical residues in the final product (Ratnaningsih et al., 2020; Faridah et al., 2022). In the AC method, starch is physically modified, which leads to starch retrogradation, thereby affecting its properties (Zhu and Liu, 2020). Retrograded starch has excellent physicochemical properties, especially thermal stability, which can improve the texture, appearance, and organoleptic properties of food. Moreover, the resistant starch (RS) content of retrograded starch can improve intestinal health (Chang et al., 2021). According to Bojarczuk et al. (2022), RS is a small fraction of starch that is resistant to degradation in the small intestine. RS is classified into five types: RS1 (physically inaccessible starch because of the cell wall barrier), RS2 (botanical source starch), RS3 (retrograded starch),

Received 21 May 2024; Revised 10 July 2024; Accepted 16 July 2024; Published online 30 September 2024
Correspondence to Eni Harmayani, E-mail: eniharmayani@ugm.ac.id

RS4 (chemically modified starch), and RS5 (amylose-lipid complexes formed during cooking). AC treatment can increase RS3 formation (Chang et al., 2021). According to Pranoto (2022), RS is a novel prebiotic, which is being used as a functional food.

A previous study showed that using a 1:1 starch-to-water ratio leads to the highest formation of RS (Abioye et al., 2018), whereas another study found that a 1:4 ratio produces optimal results (Yang et al., 2021). However, the effect of the starch-to-water ratio on RS formation of foxtail millet starch has not been reported. Therefore, the present study aimed to determine the effects of the starch-to-water ratio and number of AC cycles on the characteristics of Bengkulu foxtail millet starch, providing valuable information for the future development and use of functional ingredients in the food industry.

MATERIALS AND METHODS

Starch isolation

Foxtail millet (*Setaria italica* (L.) P. Beauv.) was sourced from Bengkulu Province, Indonesia. Foxtail millet flour was prepared in accordance with the method of Surawan et al. (2021) with some modifications. The flour was sieved through a 60-mesh sieve to obtain particles with a size of 0.25 mm. Subsequently, the flour was steeped with 0.3% NaOH (w/v) at a 1:5 (w/v) ratio and stirred using a hot plate magnetic stirrer (MS-H280-Pro, DLAB Scientific Malaysia SDN. BHD.) at a temperature of 50°C± 2°C for 60 min. The starch suspension was centrifuged using the Sorvall Biofuge Primo Centrifuge (Thermo Fisher Scientific Inc.) at 1,200 *g* for 15 min to separate the residue from the supernatant. The brownish top layer on the residue was removed, and the entire process was repeated three times. Subsequently, the residue was washed thrice with distilled water and then neutralized with 0.10 N HCl until the pH was around 7±0.20. The resulting residue was dried in a cabinet dryer (type CD5B, U. D. Rekayasa Wangdi) at 50°C for 12 h and passed through an 80-mesh sieve (0.18 mm). The yield obtained ranged from 50% to 65%. The resulting product was named "native foxtail millet starch" and stored in vacuum-sealed packaging at room temperature until further use.

AC treatment

Before AC treatment, foxtail millet starch was mixed with distilled water at different ratios (1:1 and 1:4 w/v). According to previous studies, a 1:1 ratio is an optimal condition for RS formation of Nigerian cassava starch (Abioye et al., 2018), whereas a 1:4 ratio is an optimal condition for Job's tears starch (Yang et al., 2021). The process was conducted using an autoclave (Gea YX18 LDJ, Jiangyin Binjiang Medical Equipment Co., Ltd.) at 121°C and 1 atm for 30 min, followed by cooling at room temperature (ranging from 27°C to 30°C) for 30 min. Subsequently, the starch was stored in a refrigerator (SN 118-KEG, Sanken Co.) at 4°C for 20 h. AC treatment was performed with one to three cycles for each ratio (referred to as 1:1-1C, 1:4-1C, 1:1-2C, 1:4-2C, 1:1-3C, and 1:4-3C starches). Thereafter, the starch underwent size reduction and was dried in a cabinet dryer (type CD5B, U.D. Rekayasa Wangdi) at 50°C for 8 h. Finally, the starch was ground and passed through an 80-mesh sieve (0.18 mm), resulting in autoclaved-cooled foxtail millet starch (ACFS).

Chemical analysis of foxtail millet starch

Various tests were performed in the analysis of native starch and ACFS. These tests included moisture, amylose, starch, and RS content analysis. All chemical materials used in this study were of analytical grade and obtained from Merck KgaA.

***Determination of moisture content*:** The moisture content of native starch and ACFS was determined using the thermogravimetric method International Organization for Standardization (ISO) 1666:1996 (ISO, 1996) with slight modifications, that is, using an oven (U30, Memmert GmbH & Co. KG.) at a temperature of 105°C. This heating treatment was continued until the samples reached a constant weight, indicating that the difference between weighing was less than 0.02 mg. A decrease in sample weight was considered as the amount of water in the sample.

***Determination of amylose content*:** The amylose content of native starch and ACFS was determined using the American Association of Cereal Chemistry (AACC) 61-03.01 method (AACC, 1999). Samples (100 mg) were mixed with 1 mL of 95% ethanol and 9 mL of 1 N NaOH solution. The mixture was homogenized using a vortex machine and then heated in a water bath at boiling temperature for 30 min. Then, it was homogenized again using a vortex machine (Reax Top, Heidolph Instruments GmbH & Co. KG.) and allowed to cool. Subsequently, the samples were diluted with distilled water up to 100 mL. Next, 5 mL of the sample solution was mixed with 1 mL of 1 N acetic acid solution and 2 mL of 0.01 N iodine solution and diluted with distilled water up to 100 mL. The same procedure was followed for amylose standard solutions at various concentrations (0.004, 0.008, 0.012, 0.016, and 0.020 mg/mL). Finally, the absorbance of samples and standard solutions was measured using a spectrophotometer (Genesys 10S UV-Vis, Thermo Fisher Scientific Inc.) at 620 nm, and the reagent blank was used to zero the readings.

***Determination of total starch content*:** The total starch content of native starch and ACFS was determined using the AOAC 996.11 enzymatic method with Megazyme

modification (Megazyme, 2018). This method utilizes thermostable α-amylase (K-TSTA-50A Kit, Megazyme Ltd.) to break down starch into soluble branched and unbranched maltodextrins. If required, RS was predissolved by stirring the sample with 2 M KOH at approximately 4°C, followed by neutralization with sodium acetate buffer and hydrolysis with α-amylase (K-TSTA-50A Kit, Megazyme Ltd.). Amyloglucosidase (K-TSTA-50A Kit, Megazyme Ltd.) was used to hydrolyze maltodextrins to D-glucose, which was oxidized to D-gluconate, releasing one mole of hydrogen peroxide. Then, hydrogen peroxide was quantitatively measured in a colorimetric reaction with glucose oxidase plus peroxidase reagent (GOPOD, K-TSTA-50A Kit, Megazyme Ltd.) using a spectrophotometer (Genesys 10S UV-Vis, Thermo Fisher Scientific Inc.) at 510 nm. The glucose solution standard and reagent blank were used to zero the readings. The total starch content was measured as glucose using a 0.9 conversion factor, as outlined in the total starch kit assay procedure (Megazyme, 2018).

***Determination of resistant starch (RS)*:** The RS content of native starch and ACFS was determined using the AOAC 2002-02 method by McCleary et al. (2020) with some modifications that is using an RS kit (K-RAPRS-100A, Megazyme Ltd.). This method involves digesting starch with purified α-amylase enzymes (K-RAPRS-100A, Megazyme Ltd.) at saturating levels for 4 h at 37°C to hydrolyze digestible starch into D-glucose. Ethanol was added in equal volumes to stop the reaction and separate digestible starch from RS using a centrifuge (Centro 8-BL, JP Selecta). The RS in the pellet was dissolved in 1.7 M NaOH by vigorously stirring in an ice water bath using a magnetic stirrer (MS-H280-Pro, Dlab Scientific Co., Ltd.). Then, RS was neutralized with acetate buffer. Next, RS was quantitatively hydrolyzed to D-glucose with amyloglucosidase enzyme (K-RAPRS-100A, Megazyme Ltd.) and oxidized to D-gluconate, releasing one mole of hydrogen peroxide. The RS content was equivalent to hydrogen peroxide measured in a quantitative colorimetric reaction with GOPOD reagent (K-RAPRS-100A, Megazyme Ltd.) using a spectrophotometer (Genesys 10S UV-Vis, Thermo Fisher Scientific Inc.), as outlined in the RS kit rapid assay procedure. Fourier transform infrared spectroscopy (FTIR; Nicolet^{TM} iS10, Thermo Fisher Scientific Inc.) was performed to confirm the formation of double helix bonds, which indicate RS formation.

Color measurement

In accordance with the method described by Pathare et al. (2013), the color properties of samples were measured using a chromameter (CR-400, Konica Minolta, Inc.) to determine the a*, b*, and L* (lightness) values. The chroma (C*), color difference (ΔE) value, and whiteness index (WI) were calculated using the following equations:

$$C^* = (a^2 + b^2)^{1/2} \quad \text{(Eq. 1)}$$

$$\Delta E = (\Delta a^{*2} + \Delta b^{*2} + \Delta L^*)^{1/2} \quad \text{(Eq. 2)}$$

The calculation of ΔE uses native starch as comparison starch.

$$WI = 100 - [(100 - L^*)^2 + a^{*2} + b^{*2}]^{1/2} \quad \text{(Eq. 3)}$$

(Pathare et al., 2013; Pandiselvam et al., 2023).

Measurement of the morphological properties of foxtail millet starch granules

The shape and morphological properties of foxtail millet starch granules were determined using a scanning electron microscope (SEM; JSM-6510LA, JEOL Co.) with a magnification range of ×200 – 5,000. In accordance with the method of Hadinugroho et al. (2019) with some modifications, the measurement was conducted at a voltage of 10 kV, spot size of 40, and working distance of 10 mm to obtain optimal X-ray detection. In accordance with the method of Boruczkowski et al. (2022), the average diameter and particle size of ACFS and native starch were calculated using ImageJ software for Windows 10 64-bit (IJ 154-win-java 8, National Institute of Health) at a magnification of ×50 and 200, respectively.

Analysis of the pasting properties of foxtail millet starch

The properties of starch paste were analyzed using the Rapid Visco Analyzer (RVA-4500, Perten Instrument, Perkin Elmer Co.) with Thermocline software for Windows version 3.0 (Newport Scientific Pty. Ltd.). The test was conducted using the standard RVA protocol, AACC method 76.21.01 (Castanha et al., 2021). A 10.7% starch suspension (total weight 28 g) was heated to 50°C for 1 min. Then, it was heated for 7 min until it reached a temperature of 95°C (at a rate of 6°C per minute) and maintained at that temperature for 5 min. Afterward, the sample was cooled to 50°C for 7 min at a rate of 6°C per minute and held at that temperature for 2 min.

Experimental design and data analysis

This study was conducted using a factorial design with two factors: starch-to-water ratio (1:1 and 1:4 w/v) and number of AC cycles (one, two, and three), in three replicate experiments. The results were analyzed using ANOVA to determine the effect of each factor and their interactions at a significance level of 0.05. Duncan's test was used to determine differences between treatments. Pearson correlation analysis was used to determine the correlation between parameters. All statistical analyses were conducted using SPSS software (version 25, 2017, IBM Co.).

RESULTS AND DISCUSSION

Chemical properties of foxtail millet starch

Fig. 1 shows the results of chemical analysis of ACFS and native starch, specifically the moisture, amylose, starch, and RS contents. The starch-to-water ratio had a significant effect ($P \leq 0.05$) on moisture, amylose, starch, and RS contents, whereas, the number of AC cycles only had a significant effect ($P \leq 0.05$) on starch and RS contents. However, their interaction only had a significant effect ($P \leq 0.05$) on the amylose and RS contents of ACFS and native starch.

ACFS had a significantly higher moisture content ($P \leq 0.05$) than native starch (Fig. 1A). This difference could be related to hydrogen bond formation between water and amylose and amylopectin during starch gelatinization in the autoclaving process. The hydroxyl group of starch can chemically bond with water molecules during starch gelatinization (Utama et al., 2017). Moreover, according to Popescu et al. (2022), conventional drying methods may not effectively remove water that forms hydrogen bonds with electronegative atoms, including carbohydrates, starch, pectin, fat, and protein, leading to high moisture content after drying in a cabinet dryer.

The greater the amount of distilled water added, the more significantly decreased ($P \leq 0.05$) the amylose content in AC-1 (17.89% to 8.54%), AC-2 (20.84% to 10.9%), and AC-3 (10.84% to 9.91%) (Fig. 1B). These treatments significantly reduced starch (Fig. 1C) and RS contents (Fig. 1D) ($P \leq 0.05$). The addition of more distilled water led to an increase in amylose hydrolysis, which caused the amylose content in AC treatment with a starch-to-distilled water ratio of 1:4 to be smaller than that with a ratio of 1:1. This finding was consistent with the study of Chang et al. (2021), wherein some amyloses were hydrolyzed into dextrin during the autoclaving process, depending on the heat, moisture content, and stability of the starch structure. In the present study, the 1:1-2C treatment resulted in significantly higher ($P \leq 0.05$) amylose, starch, and RS contents compared with other treatments.

The addition of more distilled water during the same number of cycles and increasing the number of AC cycles at the same starch-to-distilled water ratios significantly reduced ($P \leq 0.05$) RS formation (Fig. 1D). The highest RS formation was observed in two cycles of AC treatment with limited water addition (1:1-2C). The RS content in ACFS 1:1-2C significantly increased ($P \leq 0.05$) from 4.78% to 13.52%, which was higher than that of native starch. This increase might be related to the reassociation of retrograded amylose at 4°C. According to Chang et al. (2021), gelatinized starch changes its struc-

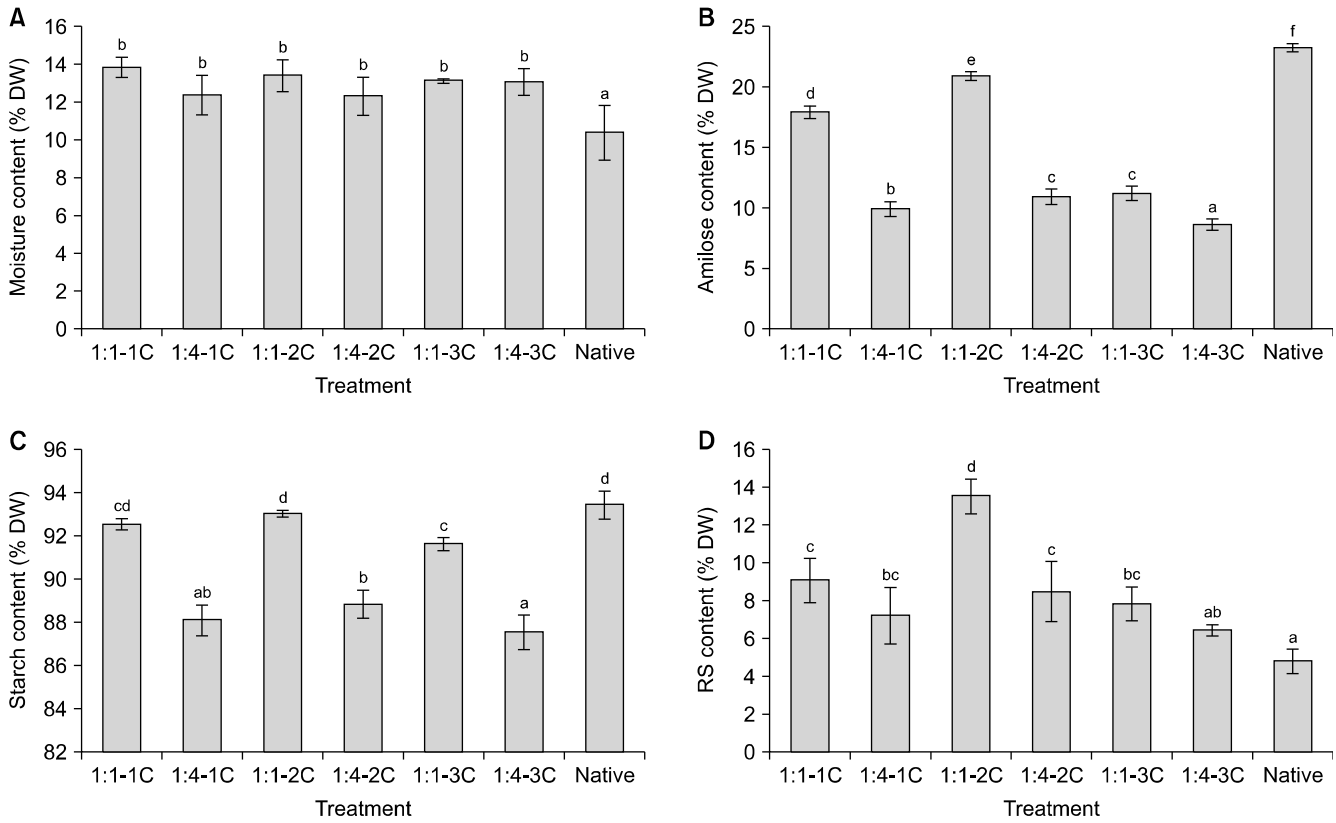

Fig. 1. Chemical properties of ACFS and native starch. (A) Moisture content, (B) amylose content, (C) starch content, and (D) RS content of ACFS and native starch. The bar represents the standard deviations from triplicate determinations. Different letters under the same parameter indicate significant differences ($P \leq 0.05$). ACFS, autoclaved-cooled foxtail millet starch; RS, resistant starch; % DW, dry weight.

ture from a semicrystalline to an amorphous state with a disordered structure. However, under cool conditions, the starch chains recombine and form a double helix structure known as retrogradation, returning to a more orderly structure. The increase in RS formation was confirmed by the formation of double helix bonds under FTIR. According to Ma and Boye (2018), the ratio in the 995/1,022 band of the FTIR spectra indicates a molecule with a double helix bond. ACFS 1:1-2C had the highest peak ratio in the 995/1,022 band (0.97), whereas native starch had the lowest peak ratio (0.79). The peak ratios for ACFS 1:4-2C and 1:4-3C were 0.92, which was lower than that of other AC treatments. Moreover, the peak ratios for ACFS 1:1-1C, 1:4-1C, and 1:1-3C were the same (0.95). The results indicated that ACFS 1:1-2C had the highest double helix formation, which is in line with RS formation. The FTIR spectra of ACFS and native starch are shown in Fig. 2.

Longton and Legrys (1981) obtained similar results when studying wheat starch with a heating (98°C) and cooling (4°C) treatment while varying the starch content (10%–80%). They found that the degree of starch recrystallization increased up to a water content of 50%, but the starch recrystallization decreased above that. The highest recrystallization was because of heating-cooling at a starch content of 50% or a ratio of 1:1 (Longton and Legrys, 1981; Chang et al., 2021). Research on cassava starch suggested that the highest RS occurred at a starch-to-water ratio of 1:1; however, the optimal formation of RS was observed during the fourth cycle (Abioye et al., 2018).

Zheng et al. (2023) found that increasing the number of AC cycles can lead to increased amylose breakdown, resulting in shorter-chain starch fractions, which affects RS formation. The optimal chain length for type-3 RS formation is α-(1-4)-D-glucan with a degree of polymerization (DP) ranging from 10 to 40. Amylose fractions with a DP below 10 or above 40 might not undergo reassociation (Schmiedl et al., 2000). This fact might help to explain why the RS formation of ACFS-3C and ACFS-1C was lower than that of ACFS-2C in the present study. According to Chang et al. (2021), more energy and time are needed to break and reassociate amylopectin chains to form double helix structures, resulting in more amylopectin requiring more AC cycles. Wiadnyani et al. (2017) and Anugrahat et al. (2015) reported that the highest increase of RS during the heating-cooling treatment occurred in the second cycle, which is consistent with the findings of the present study.

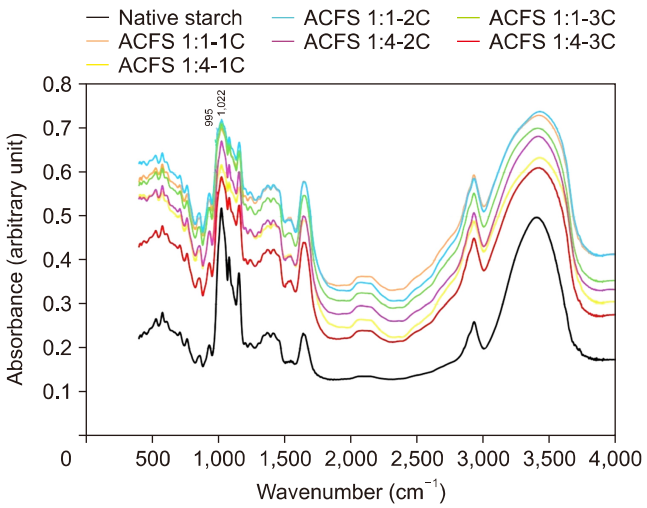

Fig. 2. Fourier transform infrared spectra of ACFS and native starch. ACFS, autoclaved-cooled foxtail millet starch.

Color properties of foxtail millet starch

The color properties (i.e., a* and b* values, L*, Wl*, C*, and ΔE) of samples were measured. The starch-to-water ratio had a significant effect ($P \leq 0.05$) on all color properties. Moreover, the number of AC cycles had a significant effect ($P \leq 0.05$) on the color properties, except for the C* value. However, their interaction only had a significant effect ($P \leq 0.05$) on the L* and Wl values of ACFS and native starch.

The results of the analysis of color properties, including a*, b*, L*, C*, ΔE, and WI, are presented in Table 1. The L* (78.24–81.54) and WI values (73.69–76.10) of ACFS were significantly lower ($P \leq 0.05$) than those of native starch. This phenomenon indicates that AC treatment decreases the L* and WI values of ACFS. This reduction could be due to the breakdown of amylose and amylopectin during the AC process, which results in shorter-chain fractions of these compounds. Repeated heating at high temperatures and pressure during the AC process led to the formation of reducing sugars. According to Kocadağlı and Gökmen (2019), the caramel color is formed by controlled pressure heating at temperatures above 120°C using raw materials such as starch, sucrose, glucose, fructose, and sugar syrup, a process known as caramelization. Color development could be related to the formation of furan derivatives from fructose or the isomerization of glucose. Additionally, the intensity of the brown color increases with higher NaCl and KCl concentrations in cereal and breakfast cereal model systems (Kocadağlı and Gökmen, 2019). This occurrence might be due to the presence of NaOH and HCl in the isolation of foxtail millet starch, which significantly reduced the L* and WI values of ACFS in general.

Chroma (C*) is a characteristic that measures the color intensity. A higher C* value indicates a more intense color (Pathare et al., 2013). The C* value of ACFS ranged from 14.42 to 15.18, which was significantly higher ($P \leq 0.05$) than that of native starch (6.10) (Table 1). This finding indicated that ACFS had a more intense color than native starch. The ΔE value of ACFS ranged from

Table 1. Color properties of autoclaved-cooled foxtail millet starch and native starch

Starch-to-distilled water ratio and cycle	L*	a*	b*	C*	WI	ΔE
1:1-1C	80.68^{c}	−3.29^{b}	14.04^{b}	14.42^{b}	75.89^{cd}	11.90^{b}
1:4-1C	80.40^{bc}	−3.32^{b}	14.11^{bc}	14.50^{b}	75.61^{c}	12.33^{bc}
1:1-2C	81.54^{d}	−3.35^{b}	14.81^{d}	15.18^{c}	76.10^{d}	11.85^{b}
1:4-2C	79.77^{b}	−3.09^{c}	14.61^{cd}	14.93^{bc}	74.86^{b}	12.87^{c}
1:1-3C	80.67^{c}	−3.62^{a}	14.68^{cd}	15.12^{c}	75.46^{c}	12.39^{bc}
1:4-3C	78.24^{a}	−3.43^{b}	14.38^{bcd}	14.78^{bc}	73.69^{a}	13.94^{d}
Native	89.08^{e}	−0.75^{d}	6.05^{a}	6.10^{a}	87.49^{e}	0.00^{a}

Data are presented as means from three replicate experiments.
Data were analyzed using one-way ANOVA followed by Duncan's post hoc test.
Different letters in the same column indicate significant differences ($P \leq 0.05$).
L*, a*, b*, C*, WI, and ΔE represent lightness, redness, yellowness, chroma, whiteness index, and total color difference, respectively.

11.85 to 13.94. According to Pathare et al. (2013), ΔE values greater than 3 signify a significant color difference compared with the reference starch. Therefore, ACFS has a notably different color than native starch.

Morphological properties of foxtail millet starch

The size properties of samples including average size area, Feret diameter, and Feret minimum diameter were measured in this study. The starch-to-water ratio and number of AC cycles had a significant effect ($P \leq 0.05$) on all size properties. However, their interaction only had a significant effect ($P \leq 0.05$) on the Feret minimum diameter. Particle sizes were obtained by analyzing images at a magnification of ×50 using ImageJ software (Table 2).

Fig. 3 shows the shapes of ACFS and native starch particles. In native foxtail millet, the starch granules exhibited a polygonal round shape with a smooth surface and were significantly smaller ($P \leq 0.05$) than ACFS particles, with an average Feret diameter of 7.86 μm. The size of ACFS was significantly greater ($P \leq 0.05$) than that of native starch, with an irregular shape and surface. This finding was consistent with that of studies conducted by Yang et al. (2021) on Job's tears starch and Ratnaningsih et al. (2020) on cowpea autoclaved-cooled starch.

According to Muñoz et al. (2015), the gelatinization and retrogradation of starch occur during the AC process. When the pasting temperature (PT) is reached, starch granules become unstable and disintegrated (gelatinized starch) (Chang et al., 2021). Consequently, the shape and surface of ACFS particles became irregular, as shown in Fig. 3 and 4. According to Chang et al. (2021), retrograded starch undergoes a process of structural reconstruction after gelatinization and cooling. SEM observations at a magnification of ×5,000 revealed that the higher water addition to starch during AC caused microstructural damage, resulting in the formation of many holes on the particle surface (Fig. 4). The particles became more porous and relatively smaller in size. The average size, Feret diameter, and Feret minimum diameter of ACFS 1:4-3C were smaller than those of other AC treatments. The more porous starch particles allowed water to penetrate the starch structure, resulting in hydrogen bonding. Thus, the starch was more easily suspended in water and rapidly gelatinized. These findings were confirmed by pasting properties using RVA (Table 3), which showed that ACFS 1:4-3C had higher viscosity and shorter gelatinization time (GT) than other AC treatments.

Pasting properties of foxtail millet starch

The pasting properties of ACFS and native starch, includ-

Table 2. Shape and size of autoclaved-cooled foxtail millet starch and native starch particles

Starch-to-distilled water ratio and cycle	Average area size (μm^2)	Feret diameter (μm)	Feret minimum diameter (μm)	Shape
1:1-1C	11,461.22^{d}	95.76^{f}	47.36^{e}	Irregular
1:4-1C	7,649.04^{bc}	78.06^{d}	36.72^{d}	Irregular
1:1-2C	10,254.42^{cd}	88.84^{e}	49.14^{e}	Irregular
1:4-2C	7,900.38^{c}	72.56^{cd}	33.40^{bc}	Irregular
1:1-3C	7,467.19^{bc}	69.89^{c}	35.13^{cd}	Irregular
1:4-3C	5,409.76^{b}	59.54^{b}	30.98^{b}	Irregular
Native	39.09^{a}	7.86^{a}	4.90^{a}	Polygonal round

Values are presented as means from three replicate experiments.
Data were analyzed using one-way ANOVA followed by Duncan's post hoc test.
Different letters in the same column indicate significant differences ($P \leq 0.05$).

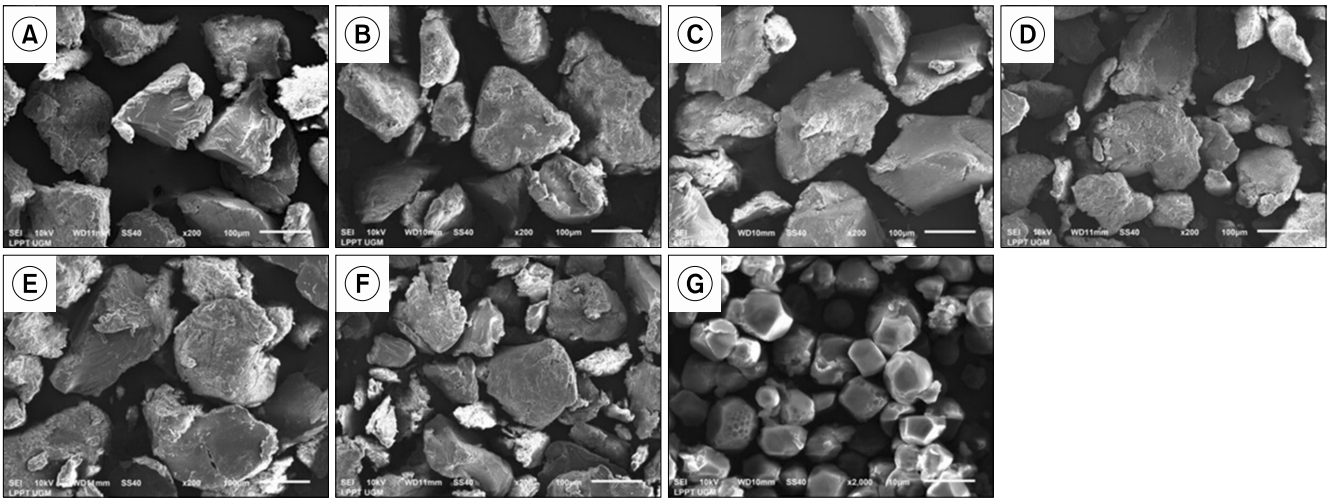

Fig. 3. Shapes of autoclaved-cooled foxtail millet starch and native starch particles visualized by scanning electron microscope at ×200 magnification. (A) 1:1-1C, (B) 1:4-1C, (C) 1:1-2C, (D) 1:4-2C, (E) 1:1-3C, (F) 1:4-3C, and (G) native starch at ×2,000 magnification.

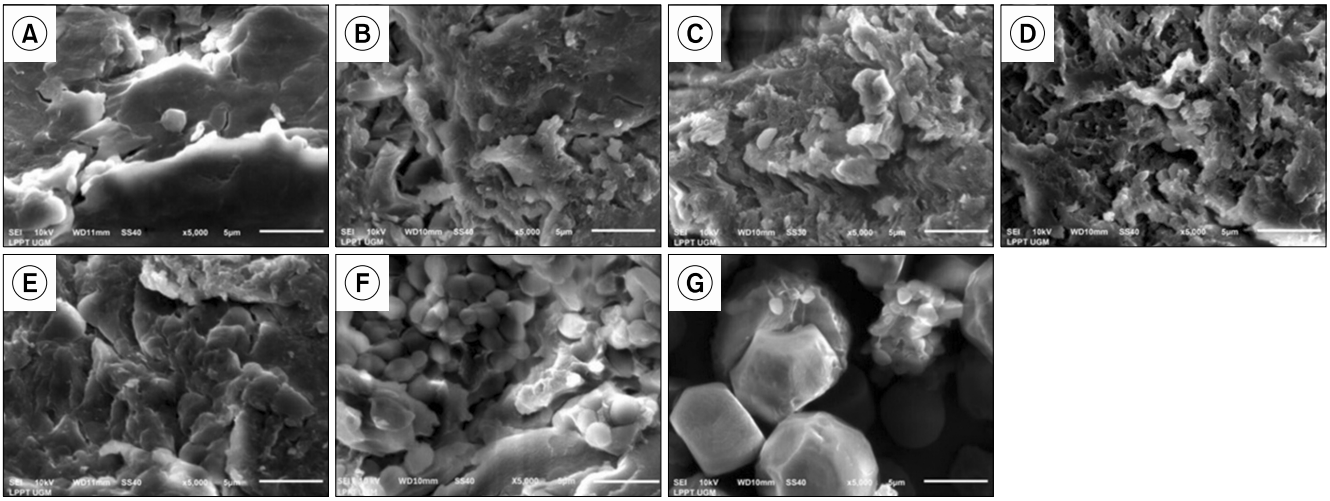

Fig. 4. Morphology of autoclaved-cooled foxtail millet starch and native starch particles visualized by scanning electron microscope at ×5,000 magnification. (A) 1:1-1C, (B) 1:4-1C, (C) 1:1-2C, (D) 1:4-2C, (E) 1:1-3C, (F) 1:4-3C, and (G) native starch.

Table 3. Pasting properties of ACFS and native starch

Starch-to-distilled water ratio and cycle	GT (min)	PT (℃)	PV (cP)	TV (cP)	BV (cP)	FV (cP)	SV (cP)
1:1-1C	6.93^{d}	59.52^{c}	3,300.33^{d}	1,888.33^{f}	1,412.00^{b}	3,147.67^{d}	1,259.33^{b}
1:4-1C	5.28^{b}	50.65^{a}	4,222.33^{f}	1,234.67^{a}	2,987.67^{e}	2,616.00^{a}	1,381.33^{e}
1:1-2C	7.62^{f}	61.95^{d}	2,437.33^{b}	2,192.00^{g}	245.33^{a}	3,332.33^{e}	1,140.33^{a}
1:4-2C	6.28^{c}	56.70^{b}	3,194.33^{c}	1,404.67^{b}	1,789.67^{c}	2,725.67^{b}	1,321.00^{c}
1:1-3C	7.31^{e}	56.42^{b}	2,025.00^{a}	1,783.00^{e}	247.33^{a}	2,922.00^{c}	1,139.00^{a}
1:4-3C	4.28^{a}	50.35^{a}	5,916.33^{g}	1,550.33^{d}	4,366.00^{f}	2,906.33^{c}	1,356.00^{d}
Native	7.61^{f}	78.58^{e}	4,138.67^{e}	1,456.00^{c}	2,682.67^{d}	2,914.33^{c}	1,458.33^{f}

Values are presented as means from three replicate experiments.
Data were analyzed using one-way ANOVA followed by Duncan's post hoc test.
Different letters in the same column indicate significant differences ($P \leq 0.05$).
GT, gelatinization time; PT, pasting temperature; PV, peak viscosity; TV, trough viscosity; BV, breakdown viscosity; FV, final viscosity; SV, setback viscosity.

ing PT, GT, peak viscosity (PV), trough viscosity (TV), breakdown viscosity (BV), final viscosity (FV), and setback viscosity (SV), were determined in this study. The starch-to-water ratio, number of AC cycles, and their interaction had a significant effect ($P \leq 0.05$) on all pasting properties.

ACFS showed a significant decrease ($P \leq 0.05$) in PT compared with native starch (Table 3). Pressure heating treatment may also cause starch depolymerization (Zheng et al., 2023). According to Chen et al. (1998), the formation of short-chain starch and damage to the crystalline areas of ACFS resulted in a lower PT (ranging from 50.35°C to 61.95°C) compared with native starch (78.58°C) due to very long branch chains. Damage to amylopectin branching in gelatinized starch produced short-chain amylopectin, which failed to form a double helix structure during retrogradation, making it easily damaged at low temperatures. This phenomenon contributes to the decrease of starch PT. In a previous study, short-chain waxy wheat starch fractions with DP of 11 – 16 exhibited damaged crystalline area compared with the longer fraction (DP 18 – 20) (Chen et al., 1998). The PT of 1:1-2C starch was significantly higher ($P \leq 0.05$) than that of other AC treatments. This finding indicates that higher temperatures are required for gelatinization and paste formation, possibly due to the formation of double helix bonds as confirmed by the FTIR spectra.

In this study, the PV value significantly decreased ($P \leq 0.05$) in AC treatment with limited water addition at one to three AC cycles compared with native starch and other treatments with higher water addition (1:4 ratio) in the same AC cycle. The decrease in the PV of ACFS with limited water addition (1:1 ratio) could indicate the more stable thermodynamic condition of the starch structure compared to other treatments with higher water addition (1:4 ratio) in the same AC cycle. According to Chang et al. (2021), repolymerization resulted in a more orderly state and stable thermodynamic condition. This was evident from the TV value, which was significantly higher ($P \leq 0.05$) in 1:1-2C starch (2,192 cP) than in other treatments. According to Balet et al. (2019), a high TV value indicates a stable paste during heating.

The BV value indicates a decrease in starch viscosity and the stability of the paste during heating. This value is obtained by subtracting the PV value from the TV value (Balet et al., 2019). The BV value of 1:1-2C starch was relatively small (245.33 cP), indicating a stable paste during heating compared with other treatments. The FV value represents starch viscosity during the cooling phase, indicating the ability of starch to form a viscous paste or gel after cooking and cooling. The FV value of 1:1-2C starch was higher (3,332.33 cP) compared with other treatments, suggesting resistance to shear forces that occurred during mixing (Balet et al., 2019).

The SV value indicates the viscosity of starch during the cooling phase and its tendency to experience retrogradation. This value is obtained by subtracting the FV value from the TV value (Braşoveanu and Nemţanu, 2020). ACFS had a lower SV value (ranging from 1,139 cP to 1,381.33 cP) than native starch (1,458.33 cP). The decrease in the SV value of ACFS compared with native starch was due to an increase in the TV value of ACFS for all treatments due to the formation of a double helix bond in ACFS. The decrease in the SV value of ACFS compared with native starch was consistent with the findings of Ratnaningsih et al. (2020) on cowpea starch and Yang et al. (2021) on Job's tears autoclaved-cooled starch.

Correlation between RS and other parameters

The results of Pearson correlation analysis, with significance levels of 0.05 and 0.001 for the parameters (chemical, color, size, and pasting properties) of ACFS and native starch, are presented in Table 4. The data indicate a positive correlation between the RS parameter and pasting properties (TV and FV), size parameters (average area, Feret diameter, and Feret minimum diameter), and color parameters (C* and ΔE values). On the other hand, the RS parameter was negatively correlated with pasting properties, including PV, BV, and SV. The L* and WI color parameters had a weak negative correlation with the RS value. The higher RS values indicated that starch tended to be more stable, which was presented by a decrease in PV, BV, and SV values. Pasting stability might be related to the formation of double helix bonds in ACFS.

Based on the results, it could be concluded that more water addition and AC cycles decreased the RS content and changed the pasting properties of foxtail millet starch. ACFS 1:1-2C had the highest RS content. Thus, it can be used as a stabilizer in heat treatment and as functional food. Meanwhile, ACFS 1:4-3C had the lowest RS content. Thus, it can be used as a thickening agent or an ingredient in instant cereal products due to its rapid GT.

ACKNOWLEDGEMENTS

The authors express their gratitude to the Deputy Head of Strengthening Research and Development at the Ministry of Research and Technology/National Research and Innovation Agency of the Republic of Indonesia for funding this study, as well as to the Universitas Gadjah Mada for providing all necessary instrument facilities and encouraging this study.

Table 4. Pearson correlation coefficient between parameters

	Moisture	Amylose	Starch	RS	L	C	WI	ΔE	Av.area	F.dia	F.min	GT	PT	PV	TV	BV	FV	SV
Moisture	1	−0.25	−0.03	0.53*	−0.69**	0.69**	−0.70**	0.69**	0.67**	0.72**	0.75**	−0.13	−0.54*	−0.21	0.48*	−0.29	0.34	−0.62**
Amylose		1	0.89**	0.24	0.77**	−0.63**	0.73**	−0.71**	−0.17	−0.31	−0.21	0.78**	0.88**	−0.30	0.47*	−0.36	0.64**	−0.00
Starch			1	0.29	0.64**	−0.45*	0.57**	−0.56**	−0.04	−0.17	−0.07	0.92**	0.77**	−0.58**	0.62**	−0.64**	0.68**	−0.32
RS				1	−0.33	0.54*	−0.42	0.44*	0.70**	0.69**	0.75**	0.33	−0.16	−0.55**	0.74**	−0.64**	0.64**	−0.73**
L					1	−0.93**	0.99**	−0.98**	−0.63**	−0.77**	−0.72**	0.61**	0.95**	−0.07	−0.08	−0.04	0.10	0.41
C						1	−0.98**	0.98**	0.75**	0.89**	0.87**	−0.35	−0.87**	−0.22	0.29	−0.26	0.07	−0.64**
WI							1	−0.99**	−0.69**	−0.83**	−0.80**	0.51*	0.93**	0.05	−0.17	0.08	0.03	0.51*
ΔE								1	0.67**	0.83**	0.80**	−0.50*	−0.93**	−0.07	0.18	−0.10	−0.03	−0.52*
Av.area									1	0.92**	0.87**	0.02	−0.50*	−0.41	0.49*	−0.46*	0.35	−0.63**
F.dia										1	0.98**	−0.11	−0.68**	−0.37	0.44*	−0.41	0.27	−0.65**
F.min											1	−0.05	−0.61**	−0.39	0.57**	−0.46*	0.41	−0.72**
GT												1	0.72**	−0.80**	0.55*	−0.81**	0.54*	−0.41
PT													1	−0.18	0.13	−0.18	0.31	0.26
PV														1	−0.55*	0.98**	−0.37	0.75**
TV															1	−0.69**	0.95**	−0.80**
BV																1	−0.53*	0.82**
FV																	1	−0.59**
SV																		1

*Correlation is significant at the 0.05 level (two-tailed).
**Correlation is significant at the 0.01 level (two-tailed).
RS, resistant starch; L, lightness; C, chroma; WI, whiteness index; ΔE, total color difference; Av.area, average area; F.dia, Feret diameter; F.min, Feret minimum diameter; GT, gelatinization time; PT, pasting temperature; PV, peak viscosity; TV, trough viscosity; BV, breakdown viscosity; FV, final viscosity; SV, setback viscosity.

FUNDING

This study received support from the Deputy Head in Strengthening Research and Development, Ministry of Research and Technology/National Research and Innovation Agency of the Republic of Indonesia, through the Doctoral Dissertation Research Scheme No 6/AMD/E1/KP.PTNBH/2020.

AUTHOR DISCLOSURE STATEMENT

The authors declare no conflict of interest.

AUTHOR CONTRIBUTIONS

Concept and design: FEDS, EH, N, DWM. Analysis and interpretation: FEDS, N, DWM. Data collection: FEDS, N, DWM. Writing the article: FEDS, EH, DWM. Critical revision of the article: FEDS, EH, N. Final approval of the article: All authors. Statistical analysis: FEDS. Obtained funding: EH, FEDS. Overall responsibility: EH, FEDS.

REFERENCES

American Association of Cereal Chemistry (AACC). Amylose content of milled rice. 1999 [cited 2022 Sep 16]. Available from: https://www.cerealsgrains.org/resources/Methods/Pages/61Rice.aspx

Abioye VF, Adeyemi IA, Akinwande BA, Kulakow P, Maziya-Dixon B. Effect of autoclaving on the formation of resistant starch from two Nigeria Cassava (*Manihot esculenta*) varieties. Food Res. 2018. 2:468-473.

Anugrahat NA, Pranoto Y, Marsono Y, Marseno DW. In vitro digestibility of indonesian cooked rice treated with cooling-reheating process and coconut milk addition. Int Res J Biol Sci. 2015. 4:34-39.

Babu AS, Mohan RJ, Parimalavalli R. Effect of single and dual-modifications on stability and structural characteristics of foxtail millet starch. Food Chem. 2019. 271:457-465.

Babu AS, Mohan RJ. Valorisation of resistant starch from foxtail millet for the development of gluten-free cereal bars and their quality evaluation. J Food Meas Charact. 2023. 17:1899-1908.

Balet S, Guelpa A, Fox G, Manley M. Rapid visco analyser (RVA) as a tool for measuring starch-related physiochemical properties in cereals: a review. Food Anal Methods. 2019. 12: 2344-2360.

Ballolli U, Malagi U, Yenagi N, Orsat V, Gariepy Y. Development and quality evaluation of foxtail millet [*Setaria italica* (L.)] incorporated breads. Karnataka J Agric Sci. 2014. 27:52-55.

Bangoura ML, Nsor-Atindana J, Ming ZH, Wei P, Mothibe KJ, Xue ZK. Starch functional properties and resistant starch from foxtail millet [*Setaria italica* (L.) P. Beauv] species. Pakistan J Nutr. 2012. 11:919-928.

Bhat S, Nandini C, Tippeswamy V, Prabhakar. Significance of small millets in nutrition and health-A review. Asian J Dairy Food Res. 2018. 37:35-40.

Bojarczuk A, Skąpska S, Khaneghah AM, Marszałek K. Health benefits of resistant starch: A review of the literature. J Funct Foods. 2022. 93:105094. https://doi.org/10.1016/j.jff.2022.105094

Boruczkowski T, Boruczkowska H, Drożdż W, Miszczak M, Leszczyński W. Use of ImageJ software for assessment of mechanical damage to starch granules. Processes. 2022. 10: 630. https://doi.org/10.3390/pr10040630

Braşoveanu M, Nemţanu MR. Pasting properties modeling and comparative analysis of starch exposed to ionizing radiation. Radiat Phys Chem. 2020. 168:108492. https://doi.org/10.1016/j.radphyschem.2019.108492

Castanha N, Rojas ML, Augusto PED. An insight into the pasting properties and gel strength of starches from different sources: effect of starch concentration. Sci Agropecu. 2021. 12:203-212.

Chang Q, Zheng B, Zhang Y, Zeng H. A comprehensive review of the factors influencing the formation of retrograded starch. Int J Biol Macromol. 2021. 186:163-173.

Chen YY, Mcpherson AE, Radosavljevic M, Lee V, Wong KS, Jane J. Effects of starch chemical structures on gelatinization and pasting properties. Żywn Technol Jakość. 1998. 4:63-71.

Doddamani S, Yenagi NB. Nutrient composition of pre-treated foxtail millet rice. Int J Curr Microbiol Appl Sci. 2018. 7: 1314-1322.

Doust AN, Kellogg EA, Devos KM, Bennetzen JL. Foxtail millet: a sequence-driven grass model system. Plant Physiol. 2009. 149:137-141.

Faridah DN, Silitonga RF, Indrasti D, Afandi FA, Jayanegara A, Anugerah MP. Verification of autoclaving-cooling treatment to increase the resistant starch contents in food starches based on meta-analysis result. Front Nutr. 2022. 9:904700. https://doi.org/10.3389/fnut.2022.904700

Hadinugroho W, Martodihardjo S, Fudholi A, Riyanto S. Esterification of citric acid with locust bean gum. Heliyon. 2019. 5:e02337. https://doi.org/10.1016/j.heliyon.2019.e02337

International Organization for Standardization (ISO). Starch-determination of moisture content-oven drying method. 1996 [cited 2022 Sep 16]. Available from: https://cdn.standards.iteh.ai/samples/22791/09d06398ea6d4c0a8e6d54e692e8de2e/ISO-1666-1996.pdf

Kocadağlı T, Gökmen V. Caramelization in foods: A food quality and safety perspective. In: Melton LD, Shahidi F, Varelis P, editors. Encyclopedia of Food Chemistry. Elsevier. 2019. p 18-29.

Longton J, Legrys GA. Differential scanning calorimetry studies on the crystallinity of ageing wheat starch gels. Stärke. 1981. 33:410-414.

Ma Z, Boye JI. Research advances on structural characterization of resistant starch and its structure-physiological function relationship: A review. Crit Rev Food Sci Nutr. 2018. 58: 1059-1083.

McCleary BV, McLoughlin C, Charmier LMJ, McGeough P. Measurement of available carbohydrates, digestible, and resistant starch in food ingredients and products. Cereal Chem. 2020. 97:114-137.

Megazyme. Total starch assay procedure (amyloglucosidase/α-amylase method). 2018 [cited 2021 Sep 16]. Available from: https://www.megazyme.com/documents/Assay_Protocol/K-TSTA-100A_DATA.pdf

Mishra G, Joshi DC, Kumar Panda B. Popping and puffing of cereal grains: A review. J Grain Process Storage. 2014. 1:34-46.

Miswarti M, Nurmala T, Anas A. Characterization and relationship 42 accessions of foxtail millet plant (Setaria italica L Beauv). J Pangan. 2014. 23:166-177.

Muñoz LA, Pedreschi F, Leiva A, Aguilera JM. Loss of birefringence and swelling behavior in native starch granules: Microstructural and thermal properties. J Food Eng. 2015. 152: 65-71.

Pandiselvam R, Mitharwal S, Rani P, Shanker MA, Kumar A, Aslam R, et al. The influence of non-thermal technologies on color pigments of food materials: An updated review. Curr Res Food Sci. 2023. 6:100529. https://doi.org/10.1016/j.crfs.2023.100529

Pathare PB, Opara UL, Al-Said FAJ. Colour measurement and analysis in fresh and processed foods: A review. Food Bioprocess Technol. 2013. 6:36-60.

Popescu GS, Radu F, Velciov AB, Pîrvulescu L, Cozma A, Stănciugelu MM, et al. A review: Water and methods employed for moisture determination in food. J Agroaliment Process Technol. 2022. 28:310-318.

Pranoto Y. Starch and its derivatives as potential source of prebiotics. In: Panesar PS, Anal AK, editors. Probiotics, Prebiotics and Synbiotics: Technological Advancements Towards Safety and Industrial Applications. John Wiley & Sons Ltd. 2022. p 378-406.

Ramlah, Pabendon MB, Daryono BS. Local food diversification of foxtail millet (*Setaria italica*) cultivars in West Sulawesi, Indonesia: A case study of diversity and local culture. Biodiversitas. 2020. 21:67-73.

Ratnaningsih N, Suparmo, Harmayani E, Marsono Y. Physicochemical properties, *in vitro* starch digestibility, and estimated glycemic index of resistant starch from cowpea (*Vigna unguiculata*) starch by autoclaving-cooling cycles. Int J Biol Macromol. 2020. 142:191-200.

Schmiedl D, Bäuerlein M, Bengs H, Jacobasch G. Production of heat-stable, butyrogenic resistant starch. Carbohydr Polym. 2000. 43:183-193.

Surawan FED, Harmayani E, Nurliyani N, Marseno DW. The effect of isolation method on proximate composition, pasting, and morphological properties of bencoolen foxtail millet (*Setaria Italica* (L)P. Bauv) starch. Agrosainstek. 2021. 5:114-123.

Utama CS, Sulistiyanto B, Kismiati S. The effects of water addition and steaming duration on starch composition of wheat pollard. Reaktor. 2017. 17:221-225.

Wiadnyani AAIS, Permana IDGM, Widarta IWR. Modification of taro starch with autoclaving-cooling method as a source of functional food. Sci J Food Technol. 2017. 4:94-102.

Yang Q, Liu L, Li X, Li J, Zhang W, Shi M, et al. Physicochemical characteristics of resistant starch prepared from Job's tears starch using autoclaving-cooling treatment. CYTA J Food. 2021. 19:316-325.

Zheng H, Sun Y, Zheng T, Zeng Y, Fu L, Zhou T, et al. Effects of shear emulsifying/ball milling/autoclave modification on structure, physicochemical properties, phenolic compounds, and antioxidant capacity of lotus (*Nelumbo*) leaves dietary fiber. Front Nutr. 2023. 10:1064662. https://doi.org/10.3389/fnut.2023.1064662

Zhu F, Liu P. Starch gelatinization, retrogradation, and enzyme susceptibility of retrograded starch: Effect of amylopectin internal molecular structure. Food Chem. 2020. 316:126036. https://doi.org/10.1016/j.foodchem.2019.126036